Anomalous optical saturation of low-energy Dirac states in graphene and its implication for nonlinear optics

Anomalous optical saturation of low-energy Dirac states in graphene and its implication for nonlinear optics

2D Materials

OPEN ACCESS

RECEIVED
20 July 2018

REVISED
9 April 2019

ACCEPTED FOR PUBLICATION
30 April 2019

PUBLISHED
17 May 2019

LETTER

Anomalous optical saturation of low-energy Dirac states in graphene and its implication for nonlinear optics

Behrooz Semnani[1,2,3,5], **Roland Jago**[1], **Safieddin Safavi-Naeini**[2,3], **Hamed Majedi**[2,3,4,6], **Ermin Malic**[1] and **Philippe Tassin**[1]

[1] Department of Physics, Chalmers University of Technology, Göteborg, Sweden
[2] Waterloo Institute for Nanotechnology, University of Waterloo, Waterloo, ON, Canada
[3] Department of Electrical & Computer Engineering, University of Waterloo, Waterloo, ON, Canada
[4] Perimeter Institute for Theoretical Physics (PI), Waterloo, ON, Canada
[5] Institute for Quantum Computing (IQC), University of Waterloo, Waterloo, ON, Canada
[6] Department of Physics & Astronomy, University of Waterloo, Waterloo, ON, Canada

E-mail: bsemnani@uwaterloo.ca

Keywords: graphene, nonlinear optics, kerr, optical saturation

Supplementary material for this article is available online

Abstract

We reveal that optical saturation of the low-energy states takes place in graphene for arbitrarily weak electromagnetic fields. This effect originates from the diverging field-induced interband coupling at the Dirac point. Using semiconductor Bloch equations to model the electronic dynamics of graphene, we argue that the charge carriers undergo ultrafast Rabi oscillations leading to the anomalous saturation effect. The theory is complemented by a many-body study of the carrier relaxations dynamics in graphene. It will be demonstrated that the carrier relaxation dynamics is slow around the Dirac point, which in turn leads to a more pronounced saturation. The implications of this effect for the nonlinear optics of graphene are then discussed. Our analysis shows that the conventional perturbative treatment of the nonlinear optics, i.e. expanding the polarization field in a Taylor series of the electric field, is problematic for graphene, in particular at small Fermi levels and large field amplitudes.

Graphene is a two-dimensional material made of carbon atoms in a honeycomb structure. Its reduced dimensionality and the symmetries of its crystalline structure render graphene a gapless semiconductor [1]. Graphene exhibits a wealth of exceptional properties, including a remarkably high mobility at room temperature [2], Klein tunneling and Zitterbewegung [3, 4], existence of a nonzero Berry phase, anomalous quantum Hall effect [5–7], quantum-limited intrinsic conductivity [8], and a unique Landau level structure [9, 10]. Underlying these peculiar electronic properties are its pseudo-relativistic quasiparticles that obey the massless Dirac equation [1]. As a direct consequence of their massless nature, the Dirac fermions have definite chiralities [11, 12]. Owing to the specific symmetries of the crystalline structure of graphene, the dynamics of the massless Dirac quasiparticles and their chiral character are topologically preserved—i.e. many-body induced band renormalizations as well as any moderate perturbations of the lattice will not open a gap in graphene's band structure [13]. A large number of the unusual properties of graphene are associated with the topologically protected band-crossing and the chiral dynamics of the charge carriers [3].

One major consequence of the topologically protected chirality of the charge carriers is the anomalous structure of the interband coupling mediated by an electromagnetic field. Its dipole matrix element obtained in the length gauge [14] exhibits a singularity at the degeneracy points, in contrast to ordinary (and even other gapless) semiconductors [15, 16]. This has raised some controversy regarding the treatment of the optical response of graphene [15, 17, 18]. Specifically, the perturbative treatment of the nonlinear optical response has been questioned [17, 19]. The nonlinear optical coefficients of graphene obtained by means of perturbation theory suffer from a nonresolvable singularity [15, 17]. Although substantial effort has been spent on developing comprehensive models for the nonlinear optical response of graphene [17, 19–24],

a self-consistent theoretical model that can resolve the above issue is still lacking. In addition, many experimental studies of the nonlinear optics of graphene have been reported [25–30]—some of these studies are difficult to reconcile with existing theoretical models.

In this Letter, we show that the singular nature of the interband dipole coupling has some significant physical implications: it causes the charge carriers in the vicinity of the Dirac points to undergo ultrafast Rabi oscillations accompanied by slow relaxation dynamics, which, intriguingly, yields an anomalous saturation effect. This finding necessitates revisiting the perturbative treatment of the nonlinear optical response of graphene to account for the extreme nonlinear interactions around the Dirac points. These conclusions will be reached by describing the dynamics of the charge carriers with semiconductor Bloch equations (SBEs) [31, 32].

We consider a free-standing graphene monolayer (in the xy plane) illuminated by a normally incident electromagnetic field. The monochromatic and spatially uniform optical field at the graphene layer is described by $\mathbf{E}(t) = \mathbf{E}_0 e^{i\omega t} + \text{c.c.}$, where $\mathbf{E}_0$ is parallel to the graphene plane. The light-matter interaction is considered semiclassically and the external field coupling is obtained in the length gauge [14]. For photon energies below approximately 2 eV, the electronic dynamics of the quasiparticles in the absence of external radiation is adequately described by the massless Dirac equation yielding the relativistic energy-momentum dispersion $\mathcal{E}_\mathbf{k} = \pm\hbar v_F|\mathbf{k}|$ [1], where $\mathbf{k}$ is the Bloch wave vector with respect to the Dirac point and v_F is the Fermi velocity.

The SBEs describe the coupled dynamics of the population difference $\mathcal{N}(\mathbf{k}, t)$ and the polarization (coherence) $\mathcal{P}(\mathbf{k}, t)$ in the momentum state $\mathbf{k}$. In the absence of electromagnetic radiation, the population difference relaxes to $\mathcal{N}^{eq}_\mathbf{k} = f(\hbar v_F k) - f(-\hbar v_F k)$, where $f(\mathcal{E})$ is the Fermi–Dirac distribution. An electromagnetic field drives the system out of equilibrium via the coupled intraband and interband dynamics. In a moving frame $\{\tau, \mathbf{k}'\} = \{t, \mathbf{k} - \delta\mathbf{k}(t)\}$, where $\delta\mathbf{k}$ obeys $\frac{\partial\delta\mathbf{k}}{\partial t} + \Gamma\delta\mathbf{k} = -\frac{e}{\hbar}\mathbf{E}(t)$ (Γ is a phenomenological intraband relaxation coefficient), the dynamics of the charge carriers is governed by

$$\frac{\partial\mathcal{N}(\mathbf{k}',\tau)}{\partial\tau} = -\gamma^{(1)}_{\mathbf{k}'}(\mathcal{N}(\mathbf{k}',\tau) - \mathcal{N}^{eq}_{\mathbf{k}'}) - 2\Phi(\mathbf{k}',\tau)\,\mathrm{Im}\{\mathcal{P}(\mathbf{k}',\tau)\}, \tag{1a}$$

$$\frac{\partial\mathcal{P}(\mathbf{k}',\tau)}{\partial\tau} = -\gamma^{(2)}_{\mathbf{k}'}\mathcal{P}(\mathbf{k}',\tau) + i\varpi_{\mathbf{k}'}\mathcal{P}(\mathbf{k}',\tau) + \frac{i}{2}\Phi(\mathbf{k}',\tau)\mathcal{N}(\mathbf{k}',\tau), \tag{1b}$$

where $\Phi(\mathbf{k}, t) = \frac{e\mathbf{E}\cdot\hat{\varphi}_\mathbf{k}}{\hbar k}$ is the matrix element of the external potential of the direct optical transition, and the unit vector $\hat{\varphi}_\mathbf{k}$ is defined as $\hat{\varphi}_\mathbf{k} = \hat{z}\times\mathbf{k}/k$. The frequency $\hbar\varpi_\mathbf{k} = 2\mathcal{E}_\mathbf{k}$ is the energy difference between the energy levels of the conduction and valence bands. $\gamma^{(1)}_\mathbf{k}$ and $\gamma^{(2)}_\mathbf{k}$ are k-dependent relaxation coefficients stemming from many-body effects such as electron–electron and electron–phonon interactions. It is worth pointing out that the moving frame accounts for the coherent Bloch oscillations, which play an important role in high-harmonics generation [33]. The detailed derivation of our theoretical model is provided in the supplemental material (stacks.iop.org/TDM/6/031003/mmedia)[7].

The light-graphene interaction as described by equations (1a) and (1b) can be interpreted as an ensemble of inhomogeneously broadened two-level systems (one for each $\mathbf{k}$). The last term in each of the two equations will lead to Rabi oscillations. Because of the singularity in $\Phi(\mathbf{k}', \tau)$ for $|\mathbf{k}| \to \mathbf{0}$, we can expect ultrafast Rabi oscillations around the Dirac point, which are damped by many-body interactions. The decay terms drive the two-level systems towards an equilibrium state. Since the interband coupling is strong around the Dirac point (equivalent to highly intense illumination), the effective field leaves the two-level systems in a statistical mixture of the ground and excited states with equal weights and absorption quenching takes place. Thus, the states around the Dirac points undergo a saturation effect, even when illuminated by an arbitrarily weak electromagnetic field.

This saturation behavior can be further understood by studying the steady-state solution of the SBEs, which is

$$\widetilde{\mathcal{N}}^{st}_\mathbf{k} = \mathcal{N}^{eq}_\mathbf{k}\frac{\gamma^{(1)}_\mathbf{k}}{\gamma^{(1)}_\mathbf{k} + \gamma^{(2)}_\mathbf{k}\left|\widetilde{\Phi}_\mathbf{k}\right|^2 / \left|\gamma^{(2)}_\mathbf{k} + i\Delta_\mathbf{k}\right|^2}, \tag{2}$$

where $\widetilde{\Phi}_\mathbf{k} = e\mathbf{E}_0\cdot\hat{\varphi}_\mathbf{k}/\hbar k$ is the complex phasor associated with $\Phi(\mathbf{k}, t)$. The function $\Delta_\mathbf{k} = \omega - \varpi_\mathbf{k}$ denotes the detuning of the two-level system at $\mathbf{k}$ with respect to the excitation.

Since $|\widetilde{\Phi}_\mathbf{k}|$ is arbitrarily large for small-k states, in the vicinity of the Dirac point the population $\widetilde{\mathcal{N}}_\mathbf{k}$ cannot be expanded in a Taylor series of the field $\widetilde{\Phi}$. This implies that the nonlinear optics of graphene is in principle a nonperturbative problem. Indeed, due to the singularity of the interband coupling in graphene, there is always a region around the Dirac point where graphene is optically saturated. The saturation threshold $E^{\text{sat}}_\mathbf{k}$ is given by

$$eE^{\text{sat}}_\mathbf{k} = \hbar k\sqrt{\Delta^2_\mathbf{k}\frac{\gamma^{(1)}_\mathbf{k}}{\gamma^{(2)}_\mathbf{k}} + \gamma^{(1)}_\mathbf{k}\gamma^{(2)}_\mathbf{k}}. \tag{3}$$

[7] See the supplemental material for a detailed derivation of the semiconductor Bloch equations and their solution, a discussion on the applicability of the velocity gauge, and the methodology to determine the k-dependent relaxation constants, to determine the absorption in the pump–probe experiments, and to obtain the semiperturbative nonlinear optical coefficients, including [14, 15, 35, 38–42, 43–45].

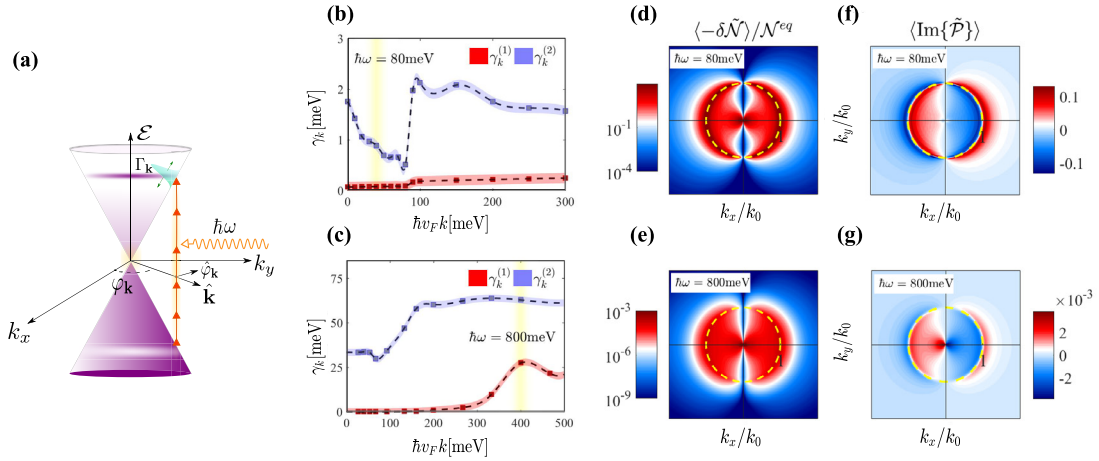

Figure 1. (a) Low-energy band structure of graphene. The angle $\hat{\varphi}_{\mathbf{k}}$ and the magnitude of the Bloch wavenumber k are defined in a polar coordinate system in reciprocal space. (b) and (c) k-dependent population and coherence relaxation coefficients shown by $\gamma_k^{(1)}$ and $\gamma_k^{(2)}$ respectively. The coefficients are calculated for $\hbar\omega = 80$ meV and 800 meV electromagnetic excitation. In both cases the electric field magnitude is 10^6 V m^{-1} and is polarized along the y-axis. (d) and (e) Relative change in the population difference with respect to the equilibrium $\delta\mathcal{N} = \mathcal{N} - \mathcal{N}_{eq}$ for $\hbar\omega = 80$ meV and 800 meV, respectively. k_0 is defined via $\hbar v_F k_0 = \hbar\omega/2$. (f) and (g) The corresponding steady-state polarization.

Saturation occurs, of course, in any two-level system at high field intensities. However, in graphene the saturation threshold field $E_{\mathbf{k}}^{\mathrm{sat}}$ is zero at the Dirac point ($k \to 0$) and, hence, there is always a region of k-space where $E_0 > E_{\mathbf{k}}^{\mathrm{sat}}$, even for arbitrarily weak intensities.

The peculiar low-threshold saturation mechanism in graphene can be quantitatively resolved using a time-domain analysis of the graphene SBEs. For the sake of comparison, this analysis has been performed for two distinct continuous excitations with optical frequency of $\hbar\omega = 80$ meV (terahertz range) and $\hbar\omega = 800$ meV (infrared), respectively. In both cases, the electric field is linearly polarized along the $\hat{y}$ direction with magnitude $E_0 = 10^6$ V m^{-1}. Graphene is assumed to be undoped here and is initially held at room temperature. The relaxation coefficients $\gamma_{\mathbf{k}}^{(1)}$ and $\gamma_{\mathbf{k}}^{(2)}$ are determined using a microscopic theory, which encompasses carrier-carrier as well as carrier-phonon scattering channels and takes into account all relevant relaxation paths including interband and intraband and even inter-valley processes [35, 36]. The reader is referred to the Supplemental Material for the details of the many-body model as well as the methodology used to extract the relaxation coefficients. The resulting relaxation coefficients are plotted in figures 1(b) and (c). We note in particular that $\gamma_{\mathbf{k}}^{(1)}$ tends to be zero around the Dirac point, which confirms the slow relaxation dynamics suggested above.

The relative change in the stationary component of the population difference due to the optical excitation as well as the amplitude of the oscillating induced polarization are shown in figures 1(d) and (e). To obtain the steady-state components, we performed Fourier analysis within a time window where the transient response has died out. As expected, a well-pronounced modified population difference around the Dirac point due to the spontaneous polarization effect (dark red region around the center) is observed. This effect is stronger for lower-frequency excitations—indeed, according to equation (3) a smaller detuning yields a weaker saturation threshold. The region in k-space where the spontaneous optical saturation is significant is well extended from the Dirac point. We note here that the size of the region depends on the applied field intensity—we will show below that this is the origin of the nonperturbative nature of the nonlinear optical response. In addition, there is, of course, the traditional optical saturation region for $\Delta_{\mathbf{k}} \approx 0$ (indicated by the yellow dashed line).

Before we continue with the importance of this anomalous optical saturation for the nonlinear optics of graphene, let us briefly make a few remarks. First, the origin of the inverse dependence of the interband transition matrix element on the wavenumber can be linked to the distinctive mathematical structure of the current operator. It is straightforward to show that the interband coupling matrix element at wavenumber $\mathbf{k}$ is $\hat{\mathbf{r}}_{cv} \approx \frac{i\hbar}{ev_F}\vec{\mathcal{J}}_{cv}(\mathbf{k})/[\mathcal{E}_c(\mathbf{k}) - \mathcal{E}_v(\mathbf{k})]$ where $\vec{\mathcal{J}}_{cv}$ is the off-diagonal element of the current operator. In contrast to ordinary semiconductors, the off-diagonal components of the current operator in graphene and other chiral materials are strictly nonzero even at the band crossing points [37]. As a direct consequence of this property of massless Dirac quasiparticles, the interband part of the position operator carries a first-order singularity at the degeneracy point. Second, one may wonder why we have not used the velocity gauge, in which optical coupling is obtained by minimal substitution $\hbar\mathbf{k} \to \hbar\mathbf{k} + e\mathbf{A}$ where $\mathbf{E} = -\partial\mathbf{A}/\partial t$. It is important to note that this approach is not gauge invariant in the 'effective Hamiltonian' picture [38–40]. We show in the supplemental material that a modification of the velocity gauge is indeed required to yield a physically correct result. This modification gives rise

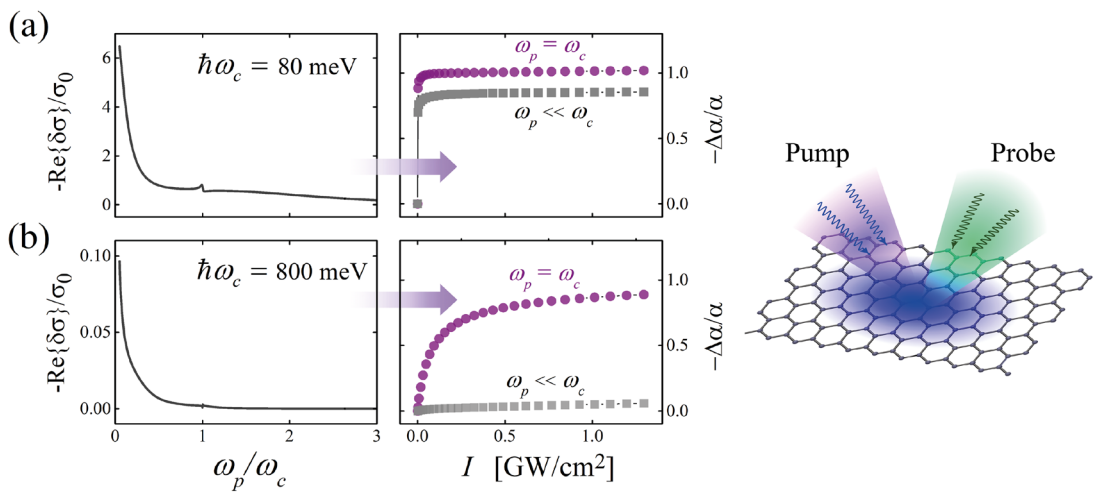

Figure 2. Change in the conductivity of graphene seen by the probe field (with frequency ω_p) in a pump–probe experiment for the pump frequencies (a) $\hbar\omega_c = 80$ meV and (b) $\hbar\omega_c = 800$ meV. The conductivity is normalized to $\sigma_0 = e^2/4\hbar$. Corresponding variations of the absorption coefficient as a function of the intensity of the pump field are shown to the right of the conductivity plots.

to the $1/k$ dependence of the interband coupling in the vicinity of the Dirac point [40]. Third, although SBEs can model the essential physics, a number of approximations have evidently been made in deriving them. For instance, for intense sub-terahertz excitations, quasi-instantaneous thermal effects can cause a population pulsation at a rate faster than the interband Rabi oscillations and thus they cannot be modelled by a spectral broadening [34]. However, owing to the fact that the anomalous saturation effect occurs around the Dirac point where the quasiparticles are off-tuned with the excitation photons, quasi-instantaneous thermal effects—taking place dominantly around the zero-detuning circle—have minimal impact on the anomalous saturation effect. Moreover, since around the Dirac point population the difference is fairly independent of temperate T, i.e. $\partial\mathcal{N}_{\mathbf{k}}^{eq}/\partial T \approx 0$, temporal fluctuations of the temperature will not significantly obscure the region where saturation happens.

We now turn to the nonlinear optics of graphene. Let us consider a nonlinear pump–probe experiment in which graphene is simultaneously subjected to a pump (ω_c) and a weaker probe (ω_p) laser beam. The conductivity tensor of graphene in the presence of the pump field and 'seen' by the probe field is calculated in the supplementary material. Figure 2 displays the change to the conductivity tensor due to the pump fields described earlier. The real part of the conductivity is related to the absorption coefficient of the probe beam via $\alpha \approx \mathrm{Re}\{\sigma\}/4\varepsilon_0 c$, where c is the speed of light in vacuum. The relative change in absorption of the probe beam is also shown in figure 2. For the 80 meV pump beam, there is strong saturation for a probe beam at the same frequency—this is because the pump beam has saturated the interband transition. For a probe beam with a much lower frequency ($\omega_p \approx \omega_c/100$), there is also strong saturation—which must be due to the unconventional effect discussed above. For the 800 meV pump, a weaker saturation is observed for a low-frequency probe. Indeed, for a higher-frequency pump the region of the low-threshold saturation is smaller (observe in equation (3) that a larger detuning results in a larger saturation field). Although the above example discusses the anomalous saturation effect for undoped graphene, the effect happens for a range of Fermi levels. Therefore, it will also be observed in samples where the charge-neutrality point fluctuates in space.

We now move on to discuss the applicability of perturbation theory in the analysis of the nonlinear response of graphene. As detailed in [15], the standard perturbative treatment of the optical response of graphene leads to a nonresolvable singularity in its higher-order nonlinear coefficients (beyond the linear response) originating from the small-$\mathbf{k}$ states. We now understand that these states should be excluded because they are saturated. However, since the saturation threshold depends on the field intensity, the nonlinear response coefficients calculated with standard perturbation theory become field dependent too. But let us investigate under what circumstances the standard nonlinear coefficients have meaning.

As mentioned earlier, neglecting the momentum of the absorbed photon, the optical transitions are vertical in k-space and, therefore, every point in the reciprocal space can be treated independently. It is argued in [15, 17, 22] that nonlinear frequency mixing in graphene can be decomposed into a number of additive contributions (see the supplemental material for a complete theoretical analysis), i.e. the nonlinear conductivity tensor is $\overline{\overline{\sigma}}^{(l)} \approx \sum_{\mathbf{k},|\mathbf{k}|>\mathbf{K}_{\mathrm{sat}}} \overline{\overline{\mathcal{I}}}_{\mathbf{k}}^{(l)}$, where K_{sat} is the radius (with respect to the Dirac point) of the spontaneously saturated region in k-space and is obtained from equation (3):

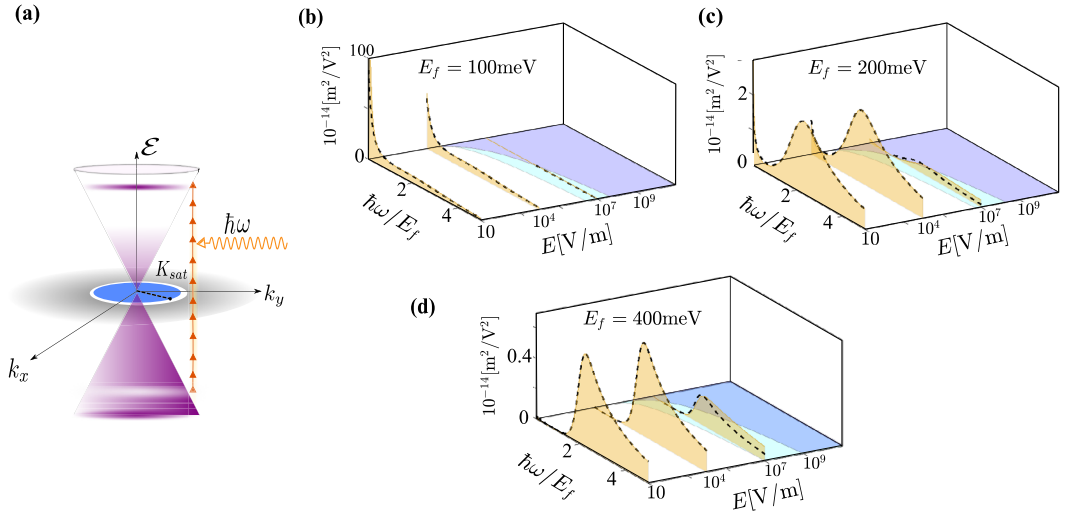

Figure 3. (a) In the calculation of the semiperturbative nonlinear coefficient, the saturated region displayed by the dark blue disc is excluded ((b)–(d)) Kerr-type nonlinearity of graphene obtained from the analytical nonperturbative approach (yellow shaded curves) and the semiperturbative approach (i.e. $|\sigma^{(3)}(\omega,\omega,-\omega)|$, black dotted curves) plotted for different field magnitudes (i.e. E). The z-axis corresponds to $|\sigma^{(3)}(\omega,\omega,-\omega)|/\sigma_0$ where $\sigma_0 = e^2/4\hbar$. The two distinctive blue shaded regions are the saturation regions in $E-\omega$ plane due to, respectively, zero-detuning (light blue) and the strong interband coupling in the vicinity of the Dirac points (dark blue). Results for different Fermi levels ($E_f = 100, 200, 400$ meV) are displayed in (b)–(d). For low Fermi levels the nonlinear optical response is noticeably field-dependent. If the photon energy lies on the dark-blue disk semiperturbative coefficients would not exist and thus the black dotted curves are not extended within the low-energy saturation domain. In the zero-detuning saturation domain (light blue area), the semiperturbative analysis fails and it cannot follow the non-perturbative results.

$$\hbar v_F K_{\mathrm{sat}} \approx \frac{1}{2}\hbar\omega - \sqrt{(\frac{1}{2}\hbar\omega)^2 - 2\hbar v_F e E_0 \sqrt{\frac{\gamma^{(2)}}{\gamma^{(1)}}}}, \tag{4}$$

and $\overline{\overline{\mathcal{I}}}^{(l)}_{\mathbf{k}}$ represents the contribution of the quasiparticles with Bloch index $\mathbf{k}$ to the l'th order nonlinear optical response. E_0 is the magnitude of the largest electric field component (most often a pump field) participating in the nonlinear process and ω is its frequency.

In order to gain insight into the intensity dependence of the nonlinear response coefficients obtained from the above-described semiperturbative approach, we compare in figure 3 the third-order nonlinear response defined as $|\sigma^{(3)}_{xxxx}(\omega,\omega,-\omega)|$ (where we have now used k-independent relaxation constants as usual) with the results of the full solution of SBEs (see the supplemental material). The yellow shaded curves display the nonperturbative solution and the black dotted curves are the results of semiperturbative approach. First, owing to the low-threshold saturation effect, there is a noticeable field dependence of the third-order nonlinear (Kerr-like) response for lower Fermi energies. When the field intensity becomes large enough to extend the saturation region to the excited k-states, the semiperturbative approach fails. As the Fermi energy becomes larger, the optically induced Pauli blocking becomes less important as the low-energy states are already Pauli blocked. It is worth pointing out that we have observed significant dependence of the results on K_{sat}. Therefore, the exact exclusion of the saturated region is necessary to achieve accurate results.

In conclusion, we have demonstrated that the topologically protected singular interband coupling in graphene leads to ultrafast Rabi oscillations, exciting the quasiparticles faster than they can relax back to the ground state. This leads to an anomalous optical saturation of the low-energy quasiparticles in graphene. Subsequently, we have shown that due to this effect the small-k states have to be excluded for the perturbative calculation of the nonlinear optical coefficients of graphene. As a result, the nonlinear coefficients obtained from perturbation theory exhibit noticeable field dependence, particularly for small Fermi levels. Although the effect revealed in this Letter has not yet been observed directly, several experiments have demonstrated the nonperturbative nature of the nonlinear optical response in graphene. For instance, [25] and [30], which present experimental results for the Kerr nonlinear coefficient of graphene obtained from z-scan measurements, demonstrate that the effective Kerr coefficient is not independent of the intensity of light. At very intense illuminations, the field dependence of the Kerr coefficient might of course have multiple origins, but this effect has been observed even in the weak-field regime, e.g. in [33, 46], which report recent experimental observations of optical and terahertz high-harmonic generation in doped and nearly-undoped graphene. Our theory provides an explanation for these experimental results indicating the nonperturbative nature of the nonlinear optics of graphene. We speculate that similar effects may be found in other Dirac materials and in Weyl semimetals.

Acknowledgments

Work at Waterloo has been supported by the Natural Science and Engineering Research Council of Canada (NSERC) and the Canada First Research Excellence Fund. Work at Chalmers has been supported by the Rune Bernhardsson Graphene fund, by Vetenskapsrådet under Grant No. 2016-03603, and by the European Union's Horizon 2020 research and innovation programme under Grant agreement No. 785219.

ORCID iDs

Behrooz Semnani https://orcid.org/0000-0002-6502-6653

References

[1] Castro Neto A H, Guinea F, Peres N M R, Novoselov K S and Geim A K 2009 *Rev. Mod. Phys.* **81** 109
[2] Bolotin K, Sikes K, Jiang Z, Klima M, Fudenberg G, Hone J, Kim P and Stormer H 2008 *Solid State Commun.* **146** 351
[3] Katsnelson M I 2006 *Eur. Phys. J.* B **51** 157
[4] Young A F and Kim P 2009 *Nat. Phys.* **5** 222
[5] Zhang Y, Tan Y-W, Stormer H L and Kim P 2005 *Nature* **438** 201
[6] Gusynin V P and Sharapov S G 2005 *Phys. Rev. Lett.* **95** 146801
[7] Gorbachev R V *et al* 2014 *Science* **346** 448
[8] Novoselov K S, Geim A K, Morozov S V, Jiang D, Katsnelson M I, Grigorieva I V, Dubonos S V and Firsov A A 2005 *Nature* **438** 197
[9] Checkelsky J G, Li L and Ong N P 2008 *Phys. Rev. Lett.* **100** 206801
[10] Mittendorff M *et al* 2014 *Nat. Phys.* **11** 75
[11] Katsnelson M I, Novoselov K S and Geim A K 2006 *Nat. Phys.* **2** 620
[12] Pal P B 2011 *Am. J. Phys.* **79** 485
[13] Bernevig B A and Hughes T L 2013 *Topological Insulators and Topological Superconductors* (Princeton, NJ: Princeton University Press)
[14] Aversa C and Sipe J E 1995 *Phys. Rev.* B **52** 14636
[15] Semnani B, Majedi A H and Safavi-Naeini S 2016 *J. Opt.* **18** 035402
[16] Kelardeh H K, Apalkov V and Stockman M I 2014 *Phys. Rev.* B **90** 085313
[17] Cheng J L, Vermeulen N and Sipe J E 2015 *Phys. Rev.* B **91** 235320
[18] Hipolito F, Taghizadeh A and Pedersen T G 2018 *Phys. Rev.* B **98** 205420
[19] Cheng J L, Vermeulen N and Sipe J E 2014 *New J. Phys.* **16** 053014
[20] Cheng J L, Vermeulen N and Sipe J E 2015 *Phys. Rev.* B **92** 235307
[21] Christensen T, Yan W, Jauho A-P, Wubs M and Mortensen N A 2015 *Phys. Rev.* B **92** 121407
[22] Mikhailov S A 2016 *Phys. Rev.* B **93** 085403
[23] Mikhailov S A 2017 *Phys. Rev.* B **95** 085432
[24] Winzer T, Mittendorff M, Winnerl S, Mittenzwey H, Jago R, Helm M, Malic E and Knorr A 2017 *Nat. Commun.* **8** 15042
[25] Zhang H, Virally S, Bao Q, Ping L K, Massar S, Godbout N and Kockaert P 2012 *Opt. Lett.* **37** 1856
[26] Chen W, Wang G, Qin S, Wang C, Fang J, Qi J, Zhang X, Wang L, Jia H and Chang S 2013 *AIP Adv.* **3** 042123
[27] Ciesielski R, Comin A, Handloser M, Donkers K, Piredda G, Lombardo A, Ferrari A C and Hartschuh A 2015 *Nano Lett.* **15** 4968
[28] Dremetsika E *et al* 2016 *Opt. Lett.* **41** 3281
[29] Vermeulen N, Castello-Lurbe D, Cheng J, Pasternak I, Krajewska A, Ciuk T, Strupinski W, Thienpont H and Erps J V 2016 *Phys. Rev. Appl.* **6** 044006
[30] Thakur S, Semnani B, Safavi-Naeini S and Hamed Majedi A 2019 (arXiv:1903.07241)
[31] Lindberg M and Koch S W 1988 *Phys. Rev.* B **38** 3342
[32] Avetissian H K, Mkrtchian G F, Batrakov K G, Maksimenko S A and Hoffmann A 2013 *Phys. Rev.* B **88** 245411
[33] Yoshikawa N, Tamaya T and Tanaka K 2017 *Science* **356** 736–8
[34] Hafez H A *et al* 2018 *Nature* **561** 507–11
[35] Malic E, Winzer T, Bobkin E and Knorr A 2011 *Phys. Rev.* B **84** 205406
[36] Malic E and Knorr A 2013 *Graphene and Carbon Nanotubes: Ultrafast Optics and Relaxation Dynamics* (New York: Wiley)
[37] Auslender M and Katsnelson M I 2007 *Phys. Rev.* B **76** 235425
[38] Virk K S and Sipe J E 2007 *Phys. Rev.* B **76** 035213
[39] Taghizadeh A, Hipolito F and Pedersen T G 2017 *Phys. Rev.* B **96** 195413
[40] Ventura G B, Passos D J, Lopes dos Santos J M B, Viana Parente Lopes J M and Peres N M R 2017 *Phys. Rev.* B **96** 035431
[41] Katsnelson M I 2012 *Graphene: Carbon in Two Dimensions* (Cambridge: Cambridge University Press)
[42] Boyd R W 2003 *Nonlinear Optics* (New York: Academic)
[43] Al-Naib I, Sipe J E and Dignam M M 2014 *Phys. Rev.* B **90** 245423
[44] Piscanec S, Lazzeri M, Mauri F, Ferrari A C and Robertson J 2004 *Phys. Rev. Lett.* **93** 185503
[45] Boyd R W and Sargent M 1988 *J. Opt. Soc. Am.* B **5** 99
[46] Bowlan P, Martinez-Moreno E, Reimann K, Elsaesser T and Woerner M 2014 *Phys. Rev.* B **89** 041408